EurJOC European Journal of Organic Chemistry

FULL PAPER

DOI: 10.1002/ejoc.201200761

Synthesis and Characterization of Dioxopyrrolopyrrole Derivatives Having Electron-Withdrawing Groups

Takuya Yamagata,[a] Junpei Kuwabara,[a] and Takaki Kanbara*[a]

Keywords: Nitrogen heterocycles / Substituent effects / Cycloaddition / Density functional calculations / Charge transfer / Electrochemistry

New dioxopyrrolopyrrole (DPP) derivatives bearing electron-withdrawing groups have been synthesized, and their photophysical properties and redox behaviors have been examined. The electron-accepting abilities of the derivatives were elucidated by cyclic voltammetry (CV) and redox titration analysis. The introduction of the electron-withdrawing groups modulated the redox properties of the DPP core, and the addition of the 1,1,4,4-tetracyanobutadiene (TCBD) moieties created a multi-redox system. The application of TD-DFT (time-dependent density functional theory) revealed the HOMO and LUMO of the compounds, and the calculation results were consistent with the photophysical and electrochemical properties of the compounds. The TCBD moieties provided the dye molecule with unique physical properties such as broad charge-transfer absorption bands and reversible multi-redox behavior.

Introduction

Dioxopyrrolopyrrole (DPP) and its derivatives were originally used as imaging colorants, surface coatings, and color filters because of their brilliant colors and high stabilities.[1] The efficient emissions of DPP derivatives are now utilized in a variety of new fields such as fluorescent molecular probes,[2] bioimaging,[3] and dye lasers.[4] As DPP derivatives have high extinction coefficients and carrier mobilities, they have also been used in the applications of organic solar cells and organic thin-film transistors (OTFTs).[5] Because the properties of DPP derivatives strongly depend on the substituents of the aromatic groups attached to the central DPP core,[1a,6] understanding the substituent effects is important for applications in optoelectronic materials.

In our previous studies, we reported the use organometallic cross-coupling reactions for the syntheses of DPP derivatives bearing electron-donating groups.[2a,6] Alternatively, the introduction of electron-withdrawing substituents, such as cyano and fluoro groups, onto the DPP structure should provide the molecule with a high electron affinity.[7–9] Indeed, it has been reported that (trifluoromethyl)-phenyl-substituted DPP derivatives can serve as n-type organic semiconductors.[5i,5j] Because a pentafluorophenyl group has electron-withdrawing ability and extends the π conjugation, its introduction onto a DPP derivative is expected to provide a molecule with a high electron affinity and result in a well-ordered stacking structure in the solid state. 1,1,4,4-Tetracyanobutadiene (TCBD) is another interesting electron-withdrawing group that can add properties to a molecule, such as a tunable CT (charge-transfer) absorption character and high electron-accepting potential.[10–12] The TCBD group can easily be introduced by a [2+2] cycloaddition reaction between tetracyanoethylene (TCNE) and electron-rich alkynes.[10] This is generally a fast, atom-economic, catalyst-free, and high-yielding reaction. Recently, Shoji et al. reported that an electrochemical reduction resulted in significant color changes to TCBD derivatives.[11] Therefore, the introduction of TCBD into dye molecules such as DPP derivatives should result in a dramatic color change when reduced.

Herein, we report the syntheses of DPP derivatives bearing electron-withdrawing components such as pentafluorophenyl and TCBD groups, and we describe the investigation of the effects of the substituents on the properties of the DPP molecules. These derivatives have been characterized by X-ray crystallography, absorption spectroscopy, emission spectroscopy, electrochemistry, and theoretical calculations.

Results and Discussion

Synthesis

Methylated DPP **1** was synthesized in 62% yield by a reaction between pigment red 254 and iodomethane in the presence of K_2CO_3 in DMF (*N*,*N*-dimethylformamide).[13] The introduction of the methyl groups to pigment red 254

[a] Tsukuba Research Center for Interdisciplinary Materials Science (TIMS), Graduate School of Pure and Applied Sciences, University of Tsukuba,
1-1-1 Tennodai, Tsukuba 305-8573, Japan
Fax: +81-29-853-4490
E-mail: kanbara@ims.tsukuba.ac.jp
Homepage: http://www.ims.tsukuba.ac.jp/~kanbara_lab/index.htm

Supporting information for this article is available on the WWW under http://dx.doi.org/10.1002/ejoc.201200761.

resulted in a molecule with good solubility in organic solvents and allowed for the product to be further functionalized by organometallic cross-coupling reactions. A palladium-catalyzed borylation of aryl chloride **1** led to aryl boronate ester **2**.[14] The reaction of compound **1** with bis(pinacolato)diboron in the presence of $Pd(OAc)_2$ with 2-(dicyclohexylphosphanyl)-2′,4′,6′-triisopropylbiphenyl (XPhos) gave compound **2** in 63% yield. A Suzuki–Miyaura coupling reaction, catalyzed by $Pd(OAc)_2$ with dicyclohexyl(2′,6′-dimethoxybiphenyl-2-yl)phosphane (SPhos)[15] as the ligand, introduced the pentafluorophenyl groups to give compound **3** in 24% yield (see Scheme 1).

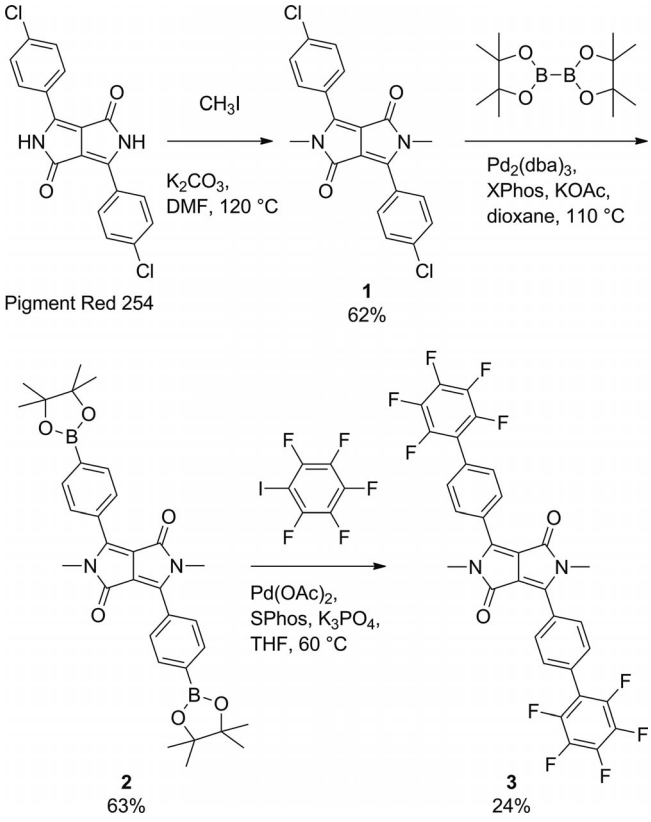

Scheme 1. Synthesis of **3**.

It has been reported that copper-free Sonogashira coupling reactions enable the use of aryl chlorides as coupling partners.[16] In accordance with this report, the reaction of compound **1** with 4-ethynyl-*N*,*N*-dimethylaniline was conducted to synthesize compound **4** (see Scheme 2). For the synthesis of a new TCBD derivative, a [2+2] cycloaddition/cycloreversion sequence of **4** with TCNE was investigated, according to the procedures described in the literature.[10b] The reaction of **4** with TCNE proceeded smoothly in CH_2Cl_2 at room temp. to give **5** in 67% yield.

Solid-State Structures

The solid-state molecular structures of **1**–**5** were examined by X-ray diffraction. The crystal structures of **1**–**5** are shown in Figure 1 and the Supporting Information. Single crystals of **3** suitable for X-ray diffraction studies were obtained by slow diffusion of hexane into a solution of the compound in $CHCl_3$. Compound **3** crystallized to form triclinic crystals with the space group $P\bar{1}$, containing two molecules with slightly different configurations in the unit cell. The structure had an inversion center at the midpoint of C-2 and C-2*. Single crystals of **5** were obtained by slowly concentrating a solution in $CHCl_3$. Compound **5** crystallized to form orthorhombic crystals with the space group *Pbca* and had an inversion center at the midpoint of C-2 and C-2*. The TCBD moieties of compound **5** were highly distorted. The torsion angle between the two dicyanovinyl planes was 66.9° in **5**. As the absolute value of this torsion angle was below 90°, the TCBD moiety adopted an *s-cis* conformation. Michinobu et al. also reported that TCBD derivatives substituted with aryl groups at both the 2- and 3-positions preferred the *s-cis* conformation.[10b]

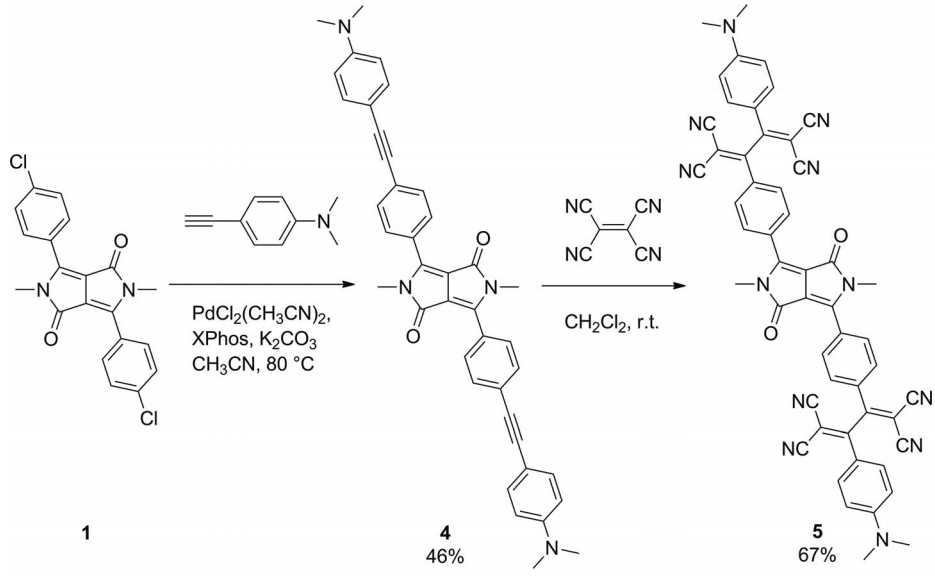

Scheme 2. Synthesis of **5**.

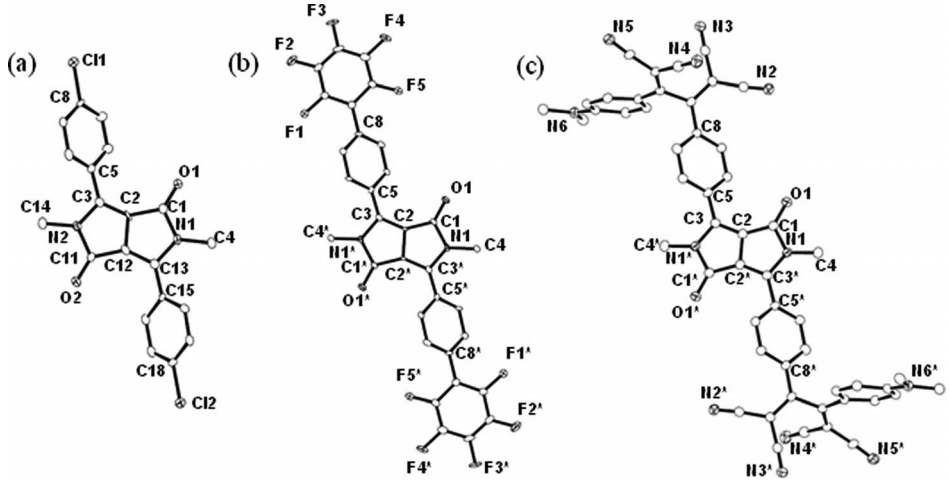

Figure 1. ORTEP drawing with thermal ellipsoids shown at the 30% probability level. (a) **1**, (b) **3**, and (c) **5**. Atoms with asterisks are crystallographically equivalent to those with the same number without an asterisk. Hydrogen atoms are omitted for clarity.

The substituents on the phenyl group affected the dihedral angle between the DPP core and the adjacent phenyl groups. Compound **4** exhibited a smaller dihedral angle (32°) than **1** (42°), **3** (40°), and **5** (42°). These results pointed to the extended conjugation of the DPP core and phenyl ring π orbitals in **4**. The electron-donating substituents increased the electron density of the phenyl rings, resulting in efficient conjugation between the DPP core and the phenyl rings.[2a]

UV/Vis Absorption Spectroscopy

The photophysical properties of compounds **1**–**5** are summarized in Table 1. The UV/Vis absorption spectra were measured in $CHCl_3$ (see Figure 2). The molar absorbance coefficient (ε) of **4** (4.32×10^4 L mol^{-1} cm^{-1}) was about double that of **1** (1.94×10^4 L mol^{-1} cm^{-1}). In addition, the absorbance maximum (λ_{max}) of **4** was at a longer wavelength than that of **1**. As the electron-donating ability of the substituents caused a redshift in the λ_{max} value,[6] the difference between the λ_{max} values was attributed to the effects of the electron-donating substituent. In spite of the electron-withdrawing ability of the pentafluorophenyl groups, the λ_{max} value of **3** was larger than that of chlorophenyl-substituted compound **1**. The results signified that the introduction of pentafluorophenyl groups extended the π conjugation. The absorption spectra of the TCBD-substituted compound **5** showed two broad bands with maxima at 461 and 535 nm. To understand the nature of the electronic transitions of compound **5**, a series of TD-DFT (time-dependent density functional theory) calculations were conducted on the optimized geometry of the compounds.

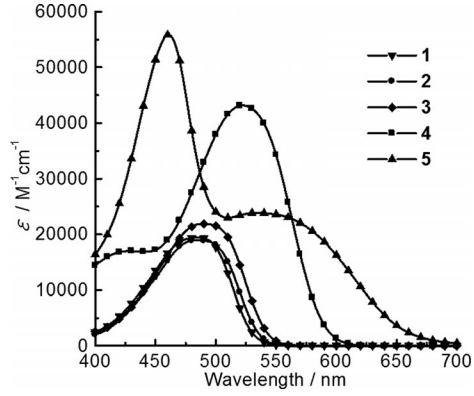

Figure 2. UV/Vis absorption spectra of **1**–**5** in $CHCl_3$.

TD-DFT Calculations

To elucidate the relationship between the substituents and the absorption spectra, compounds **1**, **3**, and **5** were examined by performing theoretical calculations.[17] After

Table 1. Photophysical properties of **1**–**5**.

Compound	UV[a]		PL in solution[a]	Excitation	Stokes shift in	Φ_f[c]
	λ_{max} [nm]	ε [L mol^{-1} cm^{-1}]	(λ_{em} [nm])[b]	spectra [nm]	solution [cm^{-1}]	in solution[a]
1	485	19400	533	472	1857	0.87
2	485	19000	543	483	2074	0.87
3	490	21900	551	493	2259	0.86
4	522	43200	619	538	3002	0.72
5	461, 535	54500, 23900	541	526	207.2	<0.01

[a] Absolute fluorescence quantum yields in chloroform. [b] Emission spectra were measured with excitation spectra (PL = photoluminescence). [c] Fluorescence quantum yields were measured with excitation at λ_{max} in UV/Vis absorption.

the optimization of the geometric structures, time-dependent density functional theory calculations were performed at the B3LYP level with the 6-31G basis set implemented in the Gaussian 03 program suite.[18,19] As shown in Figure 3, the HOMO of **5** was localized at the DPP core, whereas the LUMO of **5** covered the DPP core and one of the dicyanovinyl moieties. Table 2 summarizes the main electronic excitations with the composition, oscillator strengths, and assignments for **5**. The results of the TD-DFT calculations indicated that compound **5** had two main transitions in the long wavelength region. One of the two transitions was from the HOMO to the LUMO (f = 0.318), which was assigned to the π-π* transition of the DPP core. The other was the transition from the HOMO-2 to the LUMO (f = 0.371), which was assigned to the intramolecular charge-transfer (ICT) absorption from the *N*,*N*-dimethylanilino groups to the TCBD moieties and the DPP core. On the basis of the energy band gap, these transitions corresponded to the absorptions at 626 and 604 nm in the theoretical calculations. From the results, the broad, experimentally observed absorption around 535 nm was considered to include the two aforementioned transitions. The theoretically predicted absorption wavelength of compound **5** corresponded to a wavelength longer than the one corresponding to experimental values. This was due to various factors (such as solvent effects) that were not taken into account in the theoretical calculations.

Table 2. List of calculated electronic transitions of **5** in the gas phase.

Calcd. for **5** [nm]	Composition		f[a]
626	HOMO → LUMO HOMO–1 → LUMO+1 HOMO–2 → LUMO	(0.47) (–0.13) (–0.46)	0.318
604	HOMO–2 → LUMO HOMO–1 → LUMO+1 HOMO → LUMO	(0.49) (–0.11) (0.42)	0.371
387	HOMO–1 → LUMO+3	(0.64)	0.691

[a] Oscillator strengths.

The HOMO and LUMO energy levels of **1**, **3**, and **5** are summarized in Table 3. Although both the HOMO and LUMO of **5** were at lower energy levels than those of **1**, the difference in the LUMOs between **1** and **5** was more significant (0.79 eV) than that between their HOMOs (0.34 eV). Therefore, the TCBD moieties strongly affected the LUMO, resulting in the narrow energy band gap. The LUMO of **3** was also lower than that of **1**. This result indicated that the fluoro group on the phenyl ring provided DPP with a low-lying LUMO. The optical band gaps of **1**, **3**, and **5** from the absorption edges are 2.32, 2.09, and 1.88 eV, respectively. The trend of band gaps (**1** > **3** > **5**) was consistent with the results from the DFT calculations

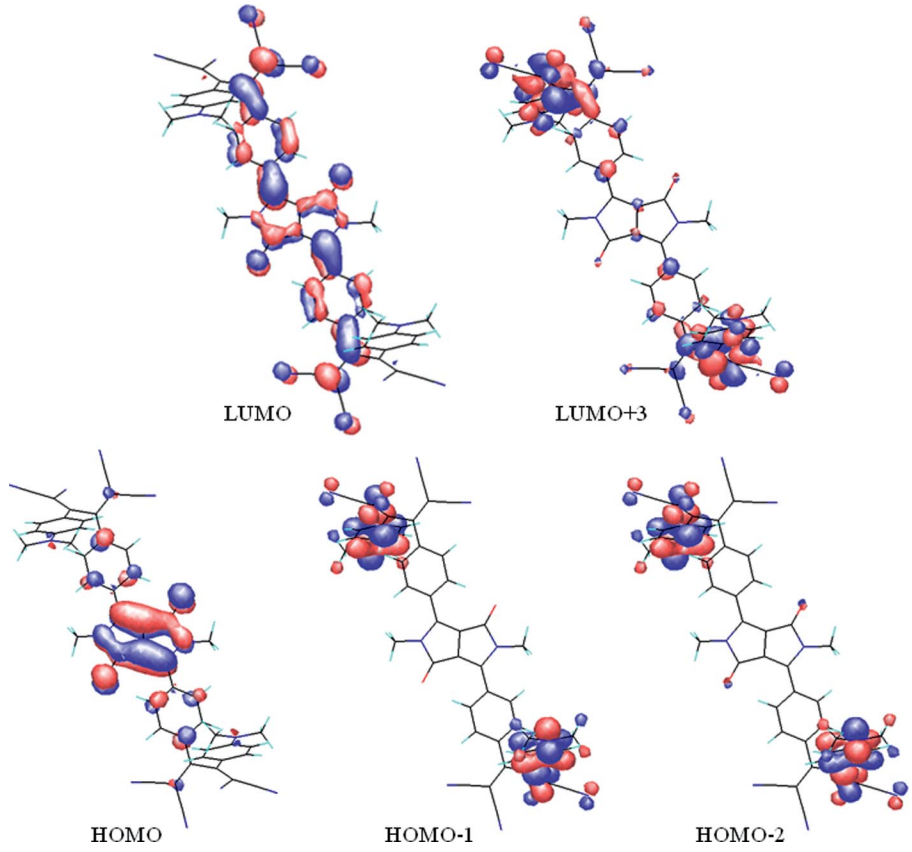

Figure 3. Molecular orbitals of compound **5**.

(see Table 3). However, the values of optical band gap are somewhat smaller than the calculated values, presumably because of the effects of solvent.

Table 3. HOMO–LUMO energies and energy band gap of **1**, **3**, and **5** on the basis of the TD-DFT calculations.

Compound	HOMO [eV]	LUMO [eV]	Band gap [eV]
1	–5.58	–2.91	2.67
3	–5.63	–3.10	2.53
5	–5.92	–3.70	2.22

Emission Spectra

The emission spectra of compounds **1**–**5** are shown in Figure 4. The photophysical data are also included in Table 1. The dependence of the maximum emission wavelength (λ_{em}) on the substituents was similar to that of the maximum absorption wavelength (**1** < **3** < **4**). The maximum emission wavelength of **3** exhibited a small redshift (18 nm) when compared to the λ_{em} value of **1**. The results also supported the theory that the pentafluorophenyl groups extended the π conjugation. Among the DPP derivatives, **4** exhibited the largest redshift (86 nm). The extended π conjugation and the electron-donating ability of the *N*,*N*-dimethylanilino groups resulted in a redshift in its emission maximum.[2a,6] Compounds **1**–**4** had high fluorescence quantum yields (0.72–0.87) in solution at room temp. (see Table 1). In contrast, the TCBD-substituted compound **5** exhibited a negligible emission in solution (Φ_f < 0.01). As compound **5** exhibited a small Stokes shift, the emission spectrum partly overlapped with the absorption spectrum. An overlap between the absorption spectrum and the emission spectrum generally indicates self-absorption, and this is one of the reasons for the negligible emission. A photoinduced electron transfer from the TCBD moieties to the DPP core could also have quenched the emission.[20]

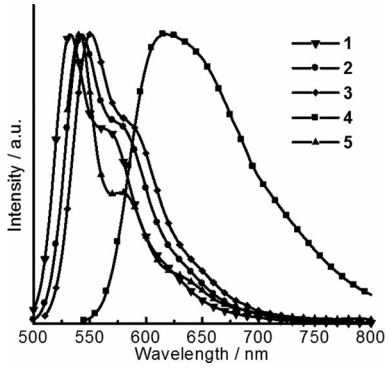

Figure 4. Normalized emission spectra of **1**–**5** in $CHCl_3$.

Electrochemistry

The introduction of electron-withdrawing substituents should enhance the electron-accepting ability of the DPP core. To elucidate the electrochemical redox behaviors, compounds **1**–**5** were evaluated by cyclic voltammetry (CV) measurements. The redox potentials of **1**–**5** are summarized in Table 4. Compounds **1**–**5** exhibited irreversible oxidation waves in the oxidation region. In contrast, compounds **1**, **3**, and **5** exhibited reversible reduction waves (see Figure 5). Compounds **2** and **4** showed a quasi-reversible reduction wave. These waves corresponded to reductions of the DPP core.[21] The reduction potential of **3** [–1.578 V vs Fc^+/Fc (ferrocenium/ferrocene)] was less negative than that of **1** (–1.638 V). This result signified that the pentafluorophenyl substituent enhanced the electron-accepting ability of the DPP core. As compound **4** with the electron-donating *N*,*N*-dimethylanilino substituent had a more negative reduction potential than those of **1**–**3**, it was clear that the substituent affected the electronic state of the DPP core through the adjacent aromatic ring.[6] Interestingly, the voltammogram of compound **5** exhibited three reversible steps at –0.88 V,

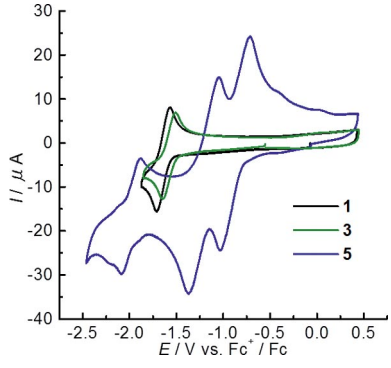

Figure 5. Cyclic voltammograms of compounds **1**, **3**, and **5** in CH_2Cl_2 (1×10^{-3} M) containing Bu_4NPF_6 (0.1 M). Sweep rate = 100 mVs^{-1}.

Table 4. Summary of electrochemical data[a] for compounds **1**–**5**.

	$E_{1/2}^{1red}$ [V][b]	$E_{1/2}^{2red}$ [V][b]	$E_{1/2}^{3red}$ [V][b]	E_{onset}^{1ox} [V][c]	E_{onset}^{1red} [V][d]	HOMO[e] [eV]	LUMO[f] [eV]
1	–1.638			0.632	–1.561	–5.43	–3.24
2	–1.625[g]			0.612	–1.554	–5.41	–3.25
3	–1.578			0.666	–1.503	–5.47	–3.30
4	–1.779[g]			0.044	–1.581	–4.84	–3.22
5	–0.878	–1.204	–1.979	0.802	–0.759	–5.60	–4.04

[a] Redox potentials were measured in CH_2Cl_2 (1×10^{-3} M) containing Bu_4NPF_6 (0.1 M). Sweep rate 100 mVs^{-1}. Potential in V vs Fc^+/Fc. [b] Half-wave potential. [c] Determined from the onset potentials of the oxidation wave. [d] Determined from the onset potentials of the reduction wave. [e] Determined from the onset potentials of the oxidation wave (vs Fc^+/Fc) using the equation (HOMO = –4.8 – E_{onset}^{1ox}). [f] Determined from the onset potentials of the reduction wave (vs Fc^+/Fc) using the equation LUMO = –4.8 – E_{onset}^{1red}. [g] Quasi-reversible redox process.

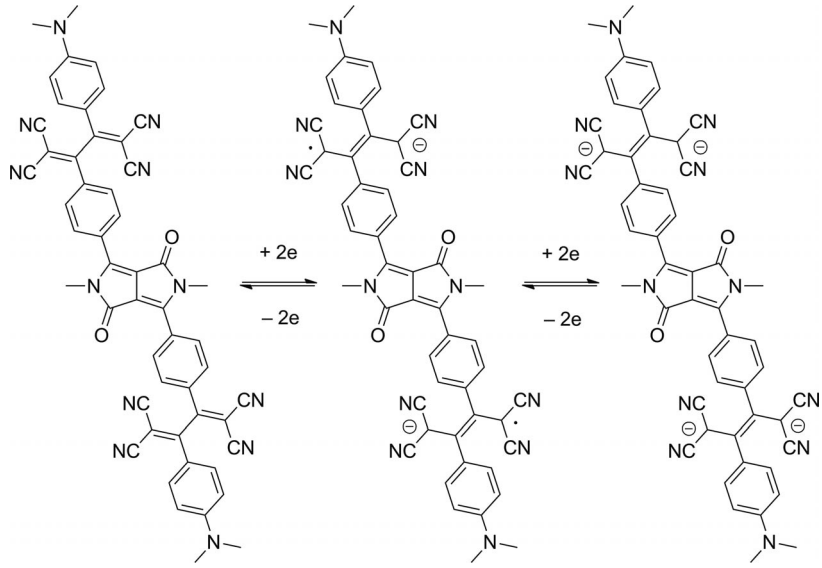

Figure 6. Redox process of compound **5**.

–1.20 V, and –1.98 V. The reduction waves at –0.88 V and –1.20 V corresponded to two-electron reductions, and the reduction wave at –1.98 V corresponded to a one-electron reduction. On the basis of the literature, the first two reduction waves were assigned to the successive reductions of the TCBD moiety.[10a] The two two-electron reductions were evidence that the two TCBD moieties in compound **5** were reduced independently (see Figure 6). The independent reduction of the TCBD moieties indicated a negligible electrochemical interaction between the TCBD moieties through the DPP core. The reduction wave at –1.98 V was assigned to the reduction of the DPP core.[12] The relatively negative reduction potential was probably due to the electron-donating effects of the dianionic TCBD moieties.

The HOMO and LUMO levels of **1**–**3** could be determined by their oxidation and reduction onset potentials, under the premise that the energy level of the ferrocene/ferrocenium couple is 4.8 eV below the vacuum level.[22] The LUMO value deduced from the electrochemistry of **3** was lower than that of **1**. This result was consistent with the results calculated by TD-DFT (see Table 3).

Redox Titration Analysis

The redox changes of **5** were accompanied by color changes. Thus, to elucidate the redox behaviors of the TCBD moieties, titrations were performed by UV/Vis spectroscopy. In the UV/Vis spectrum of **5**, the absorption bands at 461 and 535 nm decreased upon the addition of cobaltocene (Cp_2Co, $E_{1/2}$ = –1.33 V vs Fc^+/Fc, in CH_2Cl_2) with isosbestic points at 406 and 623 nm (see Figure 7). The color of the solution gradually changed from brown to red, which was accompanied by a new absorption peak at 771 nm. As compound **5** exhibited no response to ferrocene, the color change of the solution was caused by the reduction of the TCBD moieties. The formation of a tetraanionic species could account for the color change and the absorption in the near-infrared region (see Figure 6).

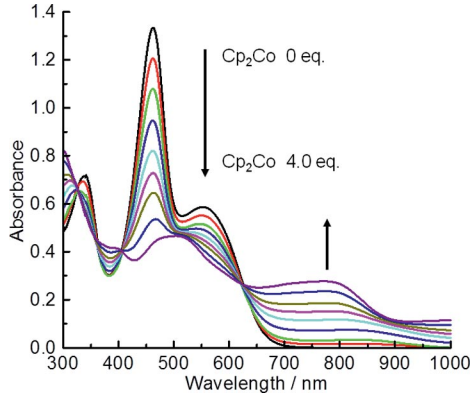

Figure 7. Changes in UV/Vis absorption spectrum of **5** in CH_2Cl_2 (2×10^{-5} M) upon addition of Cp_2Co.

Conclusions

The introduction of electron-withdrawing groups lowered the LUMO levels of the DPP derivatives and enhanced the electron-accepting abilities of the DPP core. In particular, compound **5**, bearing TCBD moieties, showed unique electrochemical responses such as a reversible five-electron reduction. Compound **5** also possessed a characteristic broad absorption band consisting of a DPP core π–π* transition and charge transfer from the TCBD moieties to the DPP core. The absorption bands could be changed by chemically reducing the TCBD moieties. As the combination of TCBD moieties on a DPP core gave rise to interesting physical properties, in the future, compound **5** could have applications in new optoelectronic materials.

Experimental Section

General Methods: NMR spectroscopic data were recorded with Bruker Avance-400, -500, and -600, JEOL EX-270, and ECS-400 NMR spectrometers. Hexafluorobenzene (δ = –164.9 ppm) was employed as an external standard in the ^{19}F NMR spectra. Elemental analyses were carried out with a Perkin–Elmer 2400 CHN Elemental Analyzer. UV/Vis spectra were recorded with a JASCO V-630iRM spectrophotometer. PL spectra were recorded with an FP-6200 spectrophotometer. Fluorescence quantum yields were obtained by a Hamamatsu Photonics absolute PL quantum yield measurement system C9920-02. MALDI mass spectra were recorded with a Kratos-Shimadzu AXIMA-CFR plus MALDI-TOF MS and Applied Biosystems SCIEX TOF/TOF™ 5800. ESI-HR mass spectra were recorded with a Waters Synapt G2.

Electrochemical Measurements: The electrochemical measurements were carried out with a standard three-electrode configuration. Bu_4NPF_6 (0.1 M solution) in dichloromethane was used as a supporting electrolyte with platinum wire auxiliary electrodes and carbon working electrodes. All of the measurements were carried out under nitrogen, and potentials were related to an Ag/Ag^+ reference electrode. The potentials were calibrated with a ferrocene/ferrocenium redox couple (Fc/Fc^+).

Computational Details: The geometrical structures were optimized at the B3LYP level for **1**, **3**, and **5** with a 6-31G basis set implemented in the Gaussian 03 program suites.[18a] Using the optimized geometries of **1**, **3**, and **5**, TD-DFT calculations were performed at the B3LYP level to predict their absorptions.

Compound 1: A suspension of pigment red 254 (1.07 mg, 3.0 mmol) and K_2CO_3 (4.56 g, 33 mmol) in DMF (50 mL) was heated at 120 °C under nitrogen. At this temperature and with vigorous stirring, a solution of methyl iodide (1.87 mL, 30 mmol) in DMF (24 mL) was added dropwise. The mixture was stirred at 120 °C for 3 h. After cooling to room temp., the mixture was diluted with $CHCl_3$ and water. The organic layer was separated and then washed with water and brine. The product was isolated by column chromatography on silica gel ($CHCl_3$) to give compound **1** (721 mg, 62%). ^1H NMR (270 MHz, $CDCl_3$): δ = 3.32 (s, 6 H), 7.49 (d, J = 8.9 Hz, 4 H), 7.83 (d, J = 8.9 Hz, 4 H) ppm. $^{13}C\{^1H\}$ NMR (100 MHz, $CDCl_3$): δ = 29.4, 109.4, 126.2, 129.2, 130.4, 137.6, 147.4, 162.4 ppm. MALDI-MS: calcd. for $C_{20}H_{15}Cl_2N_2O_2$ $[M + H]^+$ 385.1; found 385.0. $C_{20}H_{14}Cl_2N_2O_2$ (385.24): calcd. C 62.35, H 3.66, N 7.27; found C 62.00, H 3.87, N 7.26.

Compound 2: A mixture of **1** (385 mg, 1.0 mmol), bis(pinacolato)-diboron (1.78 g, 7.0 mmol), KOAc (687 mg, 7.0 mmol), $Pd_2(dba)_3$ (45.8 mg, 0.050 mmol), and XPhos (11.9 mg, 0.025 mmol) in dioxane (2.0 mL) was stirred under nitrogen at 110 °C for 4 h. After cooling to room temp., the mixture was diluted with $CHCl_3$ and water. The organic layer was separated and then washed with water and brine. The product was isolated by column chromatography on silica gel ($CHCl_3$/ethyl acetate, 10:1 → 8:1) to give compound **2** (360 mg, 63%). ^1H NMR (400 MHz, $CDCl_3$): δ = 1.37 (s, 24 H), 3.32 (s, 6 H), 7.85 (d, J = 8.4 Hz, 4 H), 7.96 (d, J = 8.4 Hz, 4 H) ppm. $^{13}C\{^1H\}$ NMR (150 MHz, $CDCl_3$): δ = 24.6, 29.4, 84.2, 109.8, 128.1, 130.3, 135.1, 148.5, 162.5 ppm. MALDI-MS: calcd. for $C_{32}H_{38}B_2N_2O_6$ $[M + H]^+$ 569.3; found 569.3. $C_{32}H_{38}B_2N_2O_6 + H_2O$ (586.30): calcd. C 65.55, H 6.88, N 4.78; found C 65.82, H 6.52, N 4.77.

Compound 3: A mixture of **2** (114 mg, 0.2 mmol), pentafluoroiodobenzene (235 mg, 0.8 mmol), K_3PO_4 (170 mg, 0.8 mmol), $Pd(OAc)_2$ (2.2 mg, 0.010 mmol), and SPhos (8.2 mg, 0.020 mmol) in THF (4.0 mL) was stirred under nitrogen at 60 °C for 22 h. After cooling to room temp., the mixture was diluted with $CHCl_3$ and water. The organic layer was separated and then washed with water and brine. The product was isolated by column chromatography on silica gel ($CHCl_3$) to give compound **3** (30.6 mg, 24%). ^1H NMR (600 MHz, $CDCl_3$): δ = 3.41 (s, 6 H), 7.63 (AA′BB′, 4 H), 8.06 (AA′BB′, 4 H) ppm. $^{13}C\{^1H\}$ NMR (150 MHz, $CDCl_3$): δ = 29.6, 110.1, 114.8–115.0 (m), 128.7, 129.4, 129.4, 130.7, 138.0 (dm, J_F = 253.1 Hz), 139.5 (dm, J_F = 182.6 Hz), 144.2 (dm, J_F = 248.7 Hz), 147.8, 162.5 ppm. ^{19}F NMR (376 MHz, $CDCl_3$): δ = –145.8 (dd, J_F = 19.2, 8.1 Hz, 4 F), –157.1 (t, J_F = 20.3 Hz, 2 F), –164.5 (m, 4 F) ppm. MALDI-MS: calcd. for $C_{32}H_{15}F_{10}N_2O_2$ $[M + H]^+$ 649.1; found 649.1. $C_{32}H_{14}F_{10}N_2O_2$ (648.45): calcd. C 59.27, H 2.18, N 4.32; found C 58.96, H 2.64, N 4.25.

Compound 4: A mixture of **1** (116 mg, 0.3 mmol), 4-ethynyl-*N*,*N*-dimethylaniline (218 mg, 1.5 mmol), Cs_2CO_3 (255 mg, 1.3 mmol), $PdCl_2(CH_3CN)_2$[23] (3.1 mg, 0.012 mmol), and XPhos (17.2 mg, 0.036 mmol) in acetonitrile (6.0 mL) was stirred under nitrogen at room temp. for 30 min. The mixture was then stirred at 80 °C for 12 h. After cooling to room temp., the mixture was diluted with $CHCl_3$ and water. The organic layer was separated and then washed with water and brine. The product was isolated by column chromatography on silica gel ($CHCl_3$/ethyl acetate, 20:1) to give compound **4** (82.9 mg, 46%). An analytically pure sample was obtained by recrystallization from a concentrated solution in $CHCl_3$. ^1H NMR (270 MHz, $CDCl_3$): δ = 3.02 (s, 12 H), 3.38 (s, 6 H), 6.68 (d, J = 8.9 Hz, 4 H), 7.44 (d, J = 8.9 Hz, 4 H), 7.63 (d, J = 8.6 Hz, 4 H), 7.91 (d, J = 8.6 Hz, 4 H) ppm. $^{13}C\{^1H\}$ NMR (100 MHz, $CDCl_3$): δ = 29.8, 40.2, 87.5, 109.3, 109.6, 111.8, 126.5, 129.0, 129.3, 130.4, 131.4, 133.0, 147.8, 150.4, 162.6 ppm. MALDI-MS: calcd. for $C_{40}H_{34}N_4O_2$ $[M]^+$ 602.3; found 602.3. $C_{40}H_{34}N_4O_2$ (602.72): calcd. C 79.71, H 5.69, N 9.30; found C 79.63, H 6.01, N 8.87.

Compound 5: TCNE (9.6 mg, 0.075 mmol) was added to a solution of **4** (15.1 mg, 0.025 mmol) in CH_2Cl_2 (1.3 mL) under nitrogen. The mixture was stirred at room temp. for 5.5 h. The solvent was removed under reduced pressure at room temp. The product was isolated by column chromatography on silica gel ($CHCl_3$/ethyl acetate, 5:1) to give compound **5** (14.3 mg, 67%). An analytically pure sample was obtained by recrystallization from a concentrated solution in $CHCl_3$. ^1H NMR (270 MHz, $CDCl_3$): δ = 3.20 (s, 12 H), 3.39 (s, 6 H), 6.76 (AA′BB′, 4 H), 7.82 (AA′BB′, 4 H), 7.88 (d, J = 8.6 Hz, 4 H), 8.09 (d, J = 8.6 Hz, 4 H) ppm. $^{13}C\{^1H\}$ NMR (150 MHz, $CDCl_3$): δ = 29.9, 40.2, 74.3, 88.5, 111.0, 111.4, 111.7, 112.5, 113.4, 114.1, 117.6, 129.9, 129.9, 130.0, 132.5, 134.0, 147.1, 154.6, 162.0, 162.3, 167.6 ppm. MALDI-MS: calcd. for $C_{52}H_{35}N_{12}O_2$ $[M + H]^+$ 859.3; found 859.3. HRMS (ESI): calcd. for $C_{52}H_{34}N_{12}O_2Na$ $[M + Na]^+$ 881.2825; found 881.2841.

Crystal Structure Analysis: Intensity data were collected with Rigaku R-AXIS Rapid and Bruker APEXII diffractometers with Mo-K_α radiation (see Table 5). The crystals were mounted on glass capillary tubes. A full-matrix least-squares refinement with anisotropic thermal parameters method by the SHELXL-97 program was used for non-hydrogen atoms. Hydrogen atoms were placed at calculated positions and were included in the structure calculations without further refinement of the parameters. CCDC-870567 (for **1**), -870568 (for **2**), -870569 (for **3**), -870570 (for **4**), and -870571 (for **5**) contain the supplementary crystallographic data for this paper. These data can be obtained free of charge from The Cambridge Crystallographic Data Centre via www.ccdc.cam.ac.uk/data_request/cif.

Supporting Information (see footnote on the first page of this article): Experimental details and characterization data of reported compounds.

Table 5. Summarized crystallographic data for compound **1**–**5**.

	1	**2**	**3**·$CHCl_3$, C_3H_7	**4**·$2CHCl_3$	**5**·$4CHCl_3$
Empirical formula	$C_{20}H_{14}Cl_2N_2O_2$	$C_{32}H_{38}B_2N_2O_6$	$C_{32}H_{14}F_{10}N_2O_2$·$CHCl_3$·C_3H_7	$C_{40}H_{34}N_4O_2$·$2CHCl_3$	$C_{52}H_{34}N_{12}O_2$·$4CHCl_3$
Formula mass	385.25	568.28	810.92	841.49	1336.43
Crystal color	yellow	orange	orange	red	black
Crystal system	monoclinic	monoclinic	triclinic	triclinic	orthorhombic
Lattice type	primitive	primitive	primitive	primitive	primitive
a [Å]	9.687(2)	10.5488(19)	9.777(6)	9.4194(13)	11.1785(5)
b [Å]	13.872(3)	11.991(2)	11.856(7)	10.9720(17)	22.7758(10)
c [Å]	12.729(3)	12.115(2)	14.401(8)	20.385(3)	23.2958(12)
α [°]			80.053(7)	77.849(4)	
β [°]	107.339(5)	108.602(4)	89.410(7)	83.644(3)	
γ [°]			85.507(7)	71.787(4)	
V [$Å^3$]	1632.8(6)	1452.4(5)	1639.1(17)	1954.1(5)	5931.1(5)
Space group	$P2_1/n$ (*#14*)	$P2_1/c$ (*#14*)	$P\bar{1}$ (*#2*)	$P\bar{1}$ (*#2*)	*Pbca* (*#61*)
Z value	4	2	2	2	4
$D_{calcd.}$ [g/cm^3]	1.567	1.299	1.643	1.430	1.497
F(000)	792	604	818	868	2712
μ (Mo-K_a) [cm^{-1}]	4.156	0.879	34.058	4.821	6.131
No. of reflections measured	total: 14717 unique: 3540 (R_{int} = 0.164)	total: 13595 unique: 3297 (R_{int} = 0.142)	total: 17938 unique: 7137 (R_{int} = 0.098)	total: 19349 unique: 8826 (R_{int} = 0.211)	total: 53663 unique: 6752 (R_{int} = 0.159)
Structure solution	direct methods (SIR92)	direct methods (SIR92)	direct methods (SIR97)	direct methods (SHELX97)	direct methods (SIR92)
No. of variables	3540	191	460	442	371
Reflection/parameter ratio	15	17.26	15.52	19.97	18.2
R_1 [$I > 2.00\sigma(I)$]	0.1571	0.1139	0.1605	0.1766	0.0825
R (all reflections)	0.2104	0.1914	0.251	0.3606	0.1459
wR_2 (all reflections)	0.4188	0.2739	0.456	0.5244	0.2573
Goodness-of-fit indicator	1.273	1.041	1.49	1.171	1.084

Acknowledgment

The authors thank the Chemical Analysis Center of the University of Tsukuba for the measurement of NMR, ESI-MS, MALDI-TOF-MS, X-ray, and elemental data. T. Y. acknowledges the University of Tsukuba Research Infrastructure Support Program for financial support. J. K. acknowledges the Foundation for Interaction in Science and Technology and the Iketani Science and Technology Foundation for financial support.

[1] a) O. Wallquist, R. Lenz, *Macromol. Symp.* **2002**, *187*, 617–629; b) Z. Hao, A. Iqbal, *Chem. Soc. Rev.* **1997**, *26*, 203–213; c) J. S. Zambounis, Z. Hao, A. Iqbal, *Nature* **1997**, *388*, 131–132; d) O. Wallquist in *High Performance Pigments* (Ed.: H. M. Smith), Wiley-VCH Verlag-GmbH, Weinheim, **2002**, pp. 159–184.

[2] a) T. Yamagata, J. Kuwabara, T. Kanbara, *Tetrahedron Lett.* **2010**, *51*, 1596–1599; b) Y. Qu, J. Hua, H. Tian, *Org. Lett.* **2010**, *12*, 3320–3323; c) L. Deng, W. Wu, H. Guo, J. Zhao, S. Ji, X. Zhang, X. Yuan, C. Zhang, *J. Org. Chem.* **2011**, *76*, 9294–9304.

[3] a) M. Y. Berezin, W. J. Akers, K. Guo, G. M. Fischer, E. Daltrozzo, A. Zumbusch, S. Achilefu, *Biophys. J.* **2009**, *97*, L22–L24; b) G. M. Fischer, C. Jüngst, M. Isomäki-Krondahl, D. Gauss, H. M. Möller, E. Daltrozzo, A. Zumbusch, *Chem. Commun.* **2010**, *46*, 5289–5291.

[4] M. Fukuda, K. Kodama, H. Yamamoto, K. Mito, *Dyes Pigm.* **2004**, *63*, 115–125.

[5] a) S. Qu, W. Wu, J. Hua, C. Kong, Y. Long, H. Tian, *J. Phys. Chem. C* **2010**, *114*, 1343–1349; b) E. Zhou, Q. Wei, S. Yamakawa, Y. Zhang, K. Tajima, C. Yang, K. Hashimoto, *Macromolecules* **2010**, *43*, 821–826; c) J. C. Bijleveld, A. P. Zoombelt, S. G. J. Mathijssen, M. M. Wienk, M. Turbiez, D. M. de Leeuw, R. A. J. Janssen, *J. Am. Chem. Soc.* **2009**, *131*, 16616–16617; d) L. Huo, J. Hou, H.-Y. Chen, S. Zhang, Y. Jiang, T. L. Chen, Y. Yang, *Macromolecules* **2009**, *42*, 6564–6571; e) Y. Zou, D. Gendron, R. Badrou-Aïch, A. Najari, Y. Tao, M. Leclerc, *Macromolecules* **2009**, *42*, 2891–2894; f) C.-Y. Yu, C.-P. Chen, S.-H. Chan, G.-W. Hwang, C. Ting, *Chem. Mater.* **2009**, *21*, 3262–3269; g) A. B. Tamayo, B. Walker, T.-Q. Nguyen, *J. Phys. Chem. C* **2008**, *112*, 11545–11551; h) M. M. Wienk, M. Turbiez, J. Gilot, R. A. J. Janssen, *Adv. Mater.* **2008**, *20*, 2556–2560; i) P. Sonar, G.-M. Ng, T. T. Lin, A. Dodabalapur, Z.-K. Chen, *J. Mater. Chem.* **2010**, *20*, 3626–3636; j) Y. Suna, J. Nishida, Y. Fujisaki, Y. Yamashita, *Chem. Lett.* **2011**, *40*, 822–824; k) Y. Qiao, Y. Guo, C. Yu, F. Zhang, W. Xu, Y. Liu, D. Zhu, *J. Am. Chem. Soc.* **2012**, *134*, 4084–4087.

[6] J. Kuwabara, T. Yamagata, T. Kanbara, *Tetrahedron* **2010**, *66*, 3736–3741.

[7] a) A. Yassar, F. Demanze, A. Jaafari, M. E. Idrissi, C. Coupry, *Adv. Funct. Mater.* **2002**, *12*, 699–708; b) Z. Bao, A. J. Lovinger, J. Brown, *J. Am. Chem. Soc.* **1998**, *120*, 207–208; c) M.-H. Yoon, S. A. DiBenedetto, A. Facchetti, T. J. Marks, *J. Am. Chem. Soc.* **2005**, *127*, 1348–1349; d) J. A. Letizia, A. Facchetti, C. L. Stern, M. A. Ratner, T. J. Marks, *J. Am. Chem. Soc.* **2005**, *127*, 13476–13477.

[8] Y. Sakamoto, T. Suzuki, M. Kobayashi, Y. Gao, Y. Fukai, Y. Inoue, F. Sato, S. Tokito, *J. Am. Chem. Soc.* **2004**, *126*, 8138–8140.

[9] a) S. Ando, J. Nishida, H. Tada, Y. Inoue, S. Tokito, Y. Yamashita, *J. Am. Chem. Soc.* **2005**, *127*, 5336–5337; b) S. Ando, R. Murakami, J. Nshida, H. Tada, Y. Inoue, S. Tokito, Y. Yamashita, *J. Am. Chem. Soc.* **2005**, *127*, 14996–14997; c) K. Takimiya, Y. Kunugi, H. Ebata, T. Otsubo, *Chem. Lett.* **2006**, *35*, 1200–1201.

[10] a) T. Michinobu, J. C. May, J. H. Lim, C. Boudon, J.-P. Gisselbrecht, P. Seiler, M. Gross, I. Biaggio, F. Diederich, *Chem. Commun.* **2005**, 737–739; b) T. Michinobu, C. Boudon, J.-P. Gisselbrecht, P. Seiler, B. Frank, N. N. P. Moonen, M. Gross, F. Diederich, *Chem. Eur. J.* **2006**, *12*, 1889–1905; c) H. Liu, J. Xu, Y. Li, Y. Li, *Acc. Chem. Res.* **2010**, *43*, 1496–1508; d) S.

Chen, Y. Li, C. Liu, W. Yang, Y. Li, *Eur. J. Org. Chem.* **2011**, 6445–6451; e) W. Zhou, J. Xu, H. Zheng, X. Yin, Z. Zuo, H. Liu, Y. Li, *Adv. Funct. Mater.* **2009**, *19*, 141–149; f) J. Xu, X. Liu, J. Lv, M. Zhu, C. Huang, W. Zhou, X. Yin, H. Liu, Y. Li, J. Ye, *Langmuir* **2008**, *24*, 4231–4237.

[11] a) T. Shoji, S. Ito, T. Okujima, N. Morita, *Eur. J. Org. Chem.* **2011**, 5134–5140; b) T. Shoji, S. Ito, K. Toyota, M. Yasunami, N. Morita, *Chem. Eur. J.* **2008**, *14*, 8398–8408; c) T. Shoji, J. Higashi, S. Ito, T. Okujima, M. Yasunami, N. Morita, *Chem. Eur. J.* **2011**, *17*, 5116–5129.

[12] S. Niu, G. Ulrich, P. Retailleau, R. Ziessel, *Org. Lett.* **2011**, *13*, 4996–4999.

[13] G. Colonna, T. Pilati, F. Rusconi, G. Zecchi, *Dyes Pigm.* **2007**, *75*, 125–129.

[14] K. L. Billingsley, T. E. Barder, S. L. Buchwald, *Angew. Chem.* **2007**, *119*, 5455; *Angew. Chem. Int. Ed.* **2007**, *46*, 5359–5363.

[15] M. R. Biscoe, T. E. Barder, S. L. Buchwald, *Angew. Chem.* **2007**, *119*, 7370; *Angew. Chem. Int. Ed.* **2007**, *46*, 7232–7235.

[16] D. Gelman, S. L. Buchwald, *Angew. Chem.* **2003**, *115*, 6175; *Angew. Chem. Int. Ed.* **2003**, *42*, 5993–5996.

[17] S. Luňák, Jr., J. Vyňuchal, M. Vala, L. Havel, R. Hrdina, *Dyes Pigm.* **2009**, *82*, 102–108.

[18] a) M. J. Frisch, G. W. Trucks, H. B. Schlegel, G. E. Scuseria, M. A. Robb, J. R. Cheeseman, J. A. Montgomery, Jr., T. Vreven, K. N. Kudin, J. C. Burant, J. M. Millam, S. S. Iyengar, J. Tomasi, V. Barone, B. Mennucci, M. Cossi, G. Scalmani, N. Rega, G. A. Petersson, H. Nakatsuji, M. Hada, M. Ehara, K. Toyota, R. Fukuda, J. Hasegawa, M. Shida, T. Nakajima, Y. Honda, O. Kitao, H. Nakai, M. Klene, X. Li, J. E. Knox, H. P. Hratchian, J. B. Cross, V. Bakken, C. Adamo, J. Jaramillo, R. Gomperts, R. E. Stratmann, O. Yazyev, A. J. Austin, R. Cammi, C. Pomelli, J. W. Ochterski, P. Y. Ayala, K. Morokuma, G. A. Voth, P. Salvador, J. J. Dannenberg, V. G. Zakrzewski, S. Dapprich, A. D. Daniels, M. C. Strain, O. Farkas, D. K. Malick, A. D. Rabuck, K. Raghavachari, J. B. Foresman, J. V. Ortiz, Q. Cui, A. G. Baboul, S. Clifford, J. Cioslowski, B. B. Stefanov, G. Liu, A. Liashenko, P. Piskorz, I. Komaromi, R. L. Martin, D. J. Fox, T. Keith, M. A. Al-Laham, C. Y. Peng, A. Nanayakkara, M. Challacombe, P. M. W. Gill, B. Johnson, W. Chen, M. W. Wong, C. Gonzalez, J. A. Pople, *Gaussian 03*, Revision D.01, Gaussian, Wallingford, CT, **2004**; b) J. P. Foster, F. Weinhold, *J. Am. Chem. Soc.* **1980**, *102*, 7211–7218; c) E. D. Glendening, A. E. Reed, J. E. Carpenter, F Weinhold, *NBO*, Version 3.1.

[19] R. Dennington, II, T. Keith, J. Millam, *GaussView*, Version 4.1, Semichem Inc., Shawnee Mission, KS, **2007**.

[20] Y. Chen, H. Wang, L. Wan, Y. Bian, J. Jiang, *J. Org. Chem.* **2011**, *76*, 3774–3781.

[21] J. Mizuguchi, A. C. Rochat, *Ber. Bunsenges. Phys. Chem.* **1992**, *96*, 708–711.

[22] B. C. Popere, A. M. D. Pelle, S. Thayumanavan, *Macromolecules* **2011**, *44*, 4767–4776.

[23] I. Abrunhosa, L. Delain-Bioton, A.-C. Gaumont, M. Gulea, S. Masson, *Tetrahedron* **2004**, *60*, 9263–9272.

Received: June 7, 2012
Published Online: ■

Dioxopyrrolopyrrole Derivatives

The redox properties of the DPP (dioxopyrrolopyrrole) core were modulated by the introduction of electron-withdrawing groups, which resulted in the enhancement of the electron-accepting ability of the DPP core. In particular, DPP derivatives with 1,1,4,4-tetracyanobutadiene (TCBD) moieties exhibited a unique electrochemical response such as undergoing a reversible five-electron reduction.

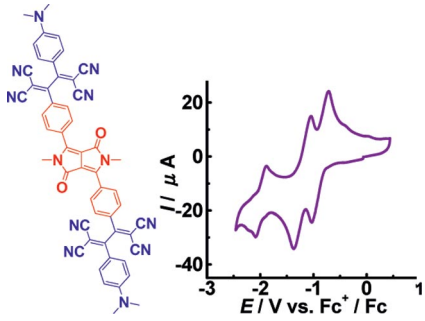

Keywords: Nitrogen heterocycles / Substituent effects / Cycloaddition / Density functional calculations / Charge transfer / Electrochemistry

